Zemani *et al.*
Journal of Engineering and Applied Science (2023) 70:99
https://doi.org/10.1186/s44147-023-00257-x

Journal of Engineering and Applied Science

REVIEWS Open Access

Simulation of CuO-water nanofluid natural convection in a U-shaped enclosure with a T-shaped baffle

Farah Zemani[1], Omar Ladjedel[2] and Amina Sabeur[1*]

*Correspondence:
sabeuramina@hotmail.com

[1] Laboratoire des Sciences Et Ingénierie Maritimes, Faculté de Génie Mécanique, Université Des Sciences Et de La Technologie d'Oran Mohamed Boudiaf Oran, B.P. 1505 Oran El-M'Naouar, 31000 Oran, Algérie
[2] Laboratoire d'Aéro-Hydrodynamique Navale, Faculté de Génie Mécanique, Université Des Sciences Et de La Technologie d'Oran Mohamed Boudiaf Oran, B.P. 1505 Oran El-M'Naouar, 31000 Oran, Algérie

Abstract

The effect of aspect ratio and baffle shape on natural convection patterns in a U-shaped cavity filled with CuO water-based nanofluid is examined in detail, with a T-shaped baffle attached to the cold wall. To solve the coupled continuity, momentum, and energy equations, a finite volume method is used, and the pressure–velocity coupling is iteratively solved with the SIMPLE algorithm. The study investigates the impact of Rayleigh number (10^4–10^6), cavity aspect ratio (Ar = 0.4, 0.6), and nanoparticle volume fraction ($0 \le \varphi \le 0.05$) on flow pattern and heat transfer features. The results are presented graphically in the form of streamlines, isotherms, mean, and local Nusselt numbers. It is observed that the mean Nusselt number increases with an increase in Rayleigh number, nanoparticle volume fraction, and aspect ratio, resulting in an improvement in heat transfer. The T-shaped baffle enhances heat transfer compared to other baffles. Though changing the aspect ratio ($0.4 \le Ar \le 0.6$) does not alter the flow pattern, an increase in Ar leads to an enhancement in the heat transfer rate.

Keywords: Nanofluid, Natural convection, Rayleigh number, U-shaped cavity, Cold rib, T-shaped baffle, Nusselt correlation

Introduction

Natural convection in cavities has been extensively researched over the years due to its frequent occurrence in various industrial applications, including heat exchangers, residential ventilation, electronic cooling devices, and solar energy collectors. Understanding the flow and heat transfer in cavities is considered a crucial research issue in computational fluid dynamics. Heat transfer fluid flow is an area of great interest, as evidenced by the numerous industrial and technological uses. Increasing convective heat transfer is the primary objective of many research efforts, and the inclusion of nanoparticles in a fluid (nanofluid) is a relevant method for achieving this. Given the problem's significance, several experimental and numerical studies [1–6] have focused on this issue in various geometrical settings.

In a study by Abu Nada et al. [7], the improved heat transfer in a differential heating chamber using Al_2O_3-water and CuO-water nanofluids was investigated. They revealed

that at high Rayleigh numbers, increasing the volume fraction of nanoparticles in CuO-water nanofluids resulted in a steady decrease in the Nusselt number. Additionally, the Nusselt number was found to be insensitive to the volume fraction at low Rayleigh numbers but was responsive to aspect ratio. A computational investigation of the natural convection cooling of a heat source encased on the bottom wall of a nanofluid-filled cavity was performed by Aminossadati et al. [8]. Their work demonstrated that adding nanoparticles to pure water improved its cooling efficiency, particularly at low Rayleigh numbers. The type of nanoparticles, as well as the length and location of the heat source, significantly affected the maximal heat source temperature. Cho et al. [9] conducted a study to investigate the natural convection heat transfer improvement of Al_2O_3-water nanofluid in a U-shaped cavity using the finite volume numerical method. Their results revealed that the average Nusselt number increased with an increase in the volume fraction of nanoparticles for all Rayleigh number values. In addition, it has been found that increasing the length of the cooled wall in a fixed heated wall length configuration can lead to improved heat transfer efficiency.

Abu Nada et al. [10] conducted a study on the natural convection heat transfer characteristics in a differential heating enclosure filled with a CuO-EG-water nanofluid for varying thermal conductivity and viscosity. The study found that the impact of viscosity models on the mean Nusselt number performance was expected to be more significant than the impact of thermal conductivity models. Additionally, the average Nusselt number decreased with an increase in the enclosure aspect ratio. However, Ghasemi et al. [11] examined numerically a natural convection heat transfer in an inclined enclosure filled with a CuO-water nanofluid. Their results showed that the inclusion of nanoparticles in pure water improved heat transfer, and the inclination angle had a significant effect on the flow and thermal fields. Similarly, Ghasemi et al. [12] investigated the effect of a magnetic field on natural convection in a square enclosure filled with AL_2O_3 nanofluid. It was found that the heat transfer performance could be improved or deteriorated with the increase of solid volume fraction depending on the values of the Hartmann number and Rayleigh number.

In a work conducted by Oztop et al. [13], natural convection in a partially heated enclosure filled with nanofluids was numerically simulated using different types of nanoparticles. Results showed that the average Nusselt number increased with the nanoparticle volume fraction across the entire range of Rayleigh numbers, as well as with an increase in the height of the heating element. Meanwhile, Srinivas Rao et al. [14] experimentally investigated the heat transfer characteristics of dilute Al_2O_3 water-based nanofluids under natural convection through an interferometric study. They found that the convective field was highly dependent on the nanofluid concentration.

Yildiz et al. [15] conducted the natural convection of CuO-water nanofluid in a U-shaped enclosure, exploring the impact of aspect ratio, nanofluid volume fractions, cavity inclination on velocity and temperature fields for $Ra = 10^5$ and $Pr = 6.2$. In another study, Yildiz et al. [16] focused on the effect of cold wall dimensions on the natural convection of CuO nanofluid in a U-shaped enclosure by investigating the impact of aspect ratio. They discovered that the vertical aspect ratio had a greater effect on heat transfer than the horizontal aspect ratio, implying that increasing the cold wall height is more effective than increasing the cold wall width for most purposes. Mohebbi

et al. [17] used the Boltzmann lattice method (LBM) to investigate thermo-gravitational convection of nanofluid inside a Γ-shaped enclosure that contains a local heater. Their results indicated that the average Nusselt number increased with Rayleigh number and nanoparticles concentration and that the enclosure aspect ratio and obstacle height had a decreasing effect.

Chamkha et al. [18] conducted a study on the influence of CuO-water nanofluid and a uniform magnetic field on natural convection and entropy generation within a C-shaped cavity, accounting for the Brownian motion phenomenon to describe the nanofluid's characteristics. Their results showed that increasing the nanoparticle volume fraction enhanced natural convection but also increased the entropy generation rate. Furthermore, the application of a magnetic field was observed to mitigate both the natural convection and entropy generation rate.

Mahalakshmi et al. [19] performed a numerical simulation of natural convection heat transfer in an enclosure containing a block heater and a nanofluid, investigating the effect of different central heater lengths on the flow and temperature fields at various Rayleigh numbers. They showed that heat transfer increased with longer heater lengths in both vertical and horizontal positions as Rayleigh number values increased. Moreover, it was found that the Ag-water nanofluid outperformed CuO-water and Al_2O_3-water nanofluids in terms of heat transfer improvement. Meanwhile, Triveni et al. [20] also investigated the natural convection of an Al_2O_3-water nanofluid in an arched enclosure through numerical analysis. Their study found that the heat transfer efficiency increased with increasing nanoparticles volume fraction up to 5% and then decreased gradually. They also observed that the heat transfer rate increased with curvature ratio and Rayleigh number.

Dutta et al. [21] conducted a numerical investigation of natural convection heat transfer in a recto-trapezoidal enclosure filled with copper–water nanofluids, with uniform heating applied to the bottom wall. Their findings indicated that the average Nusselt number increased with increasing solid volume fraction of copper–water nanoparticles, and heat transfer improved by over 20% for $Ra = 10^6$ and up to 30% for $Ra = 10^3$ with the use of Cu-water nanofluid. Snoussi et al. [22] performed a numerical analysis of convective heat transfer in three-dimensional U-shaped enclosures using nanofluids (Cu and Al_2O3). They observed that heat transfer improved with increasing nanoparticles volume fractions, Rayleigh numbers, and cooled wall length extensions. Islam et al. [23] investigated a prismatic-shaped enclosure containing a two-dimensional Cu-H_2O nanofluid with a magnetic field under MHD conditions. They concluded that natural convection heat and energy transfer was enhanced with increasing Rayleigh number and nanoparticles volume fraction but decreased with increasing Hartmann number. The results of this study could be useful in designing effective cooling systems for various mechanical chambers.

Hasan et al. [24] studied a periodic unsteady natural convection of a CNT nanopowder liquid in a triangular-shaped mechanical chamber. Their results showed that with increasing Rayleigh number, the velocity, vorticity, and magnitude of the pressure gradient became large, resulting in reduced fluid flow vortices with dimensionless time. They found also that the highest heat transfer rate was achieved using the nano liquid with a 15% concentration. A numerical investigation on a three-dimensional thermal

convection of a fluid with temperature-dependent viscosity in a porous cubic cavity was carried out by Astanina et al. [25]. They concluded that increasing the Darcy number (the permeability of the porous zone) increased the convective motion rate of the fluid and that enhancing the interphase heat transfer coefficient could result in an enhancement of heat transfer in the cube.

In their study, Kadhim et al. [26] used the local thermal no equilibrium model to numerically analyze the buoyancy-driven flow in a porous enclosure with a corrugated heated bottom wall. The enclosure was filled with Cu-Al_2O_3/water hybrid nanofluid. The findings indicated that increasing the thermal conductivity of nanoparticles led to an increase in the heat transfer rate. The maximum heat transfer rate was obtained at $\phi = 0.04$. Meanwhile, Alam et al. [27] analyzed the hydro-thermal incidents of different nanofluids occupying a quarter circular vicinity using transient natural convection. They considered water (H_2O), kerosene (Ke), and engine oil (EO) as base fluids and copper (Cu), cobalt (Co), and iron oxide (Fe_3O_4) as nanoparticles. The outcomes of their research revealed that the heat transfer rate significantly increased with higher Rayleigh number values, nanoparticle volume fraction (ϕ), and magnetic field period (λ), while increasing the Hartmann number (Ha) resulted in a decrease in the total heat transfer rate. These numerical results could prove useful in assessing the heat transfer characteristics of solar collectors and electronic devices. Additionally, Al Hajri et al. [28] investigated the impact of the Maxwell–Cattaneo (MC) effect (or hyperbolic heat flow) on the flow and heat transfer dynamics of a porous medium filled with water and crude oil in a state of local thermal no equilibrium (LTNE). The results showed a decrease in fluid friction and an increase in the rate of heat transfer in both the fluid and solid.

Hasan et al. [29] conducted a study on the unsteady laminar magnetohydrodynamic flow of convective nanofluids in a square cavity that was driven by an exothermic chemical reaction. In this study, water-based nanofluid containing iron oxide (Fe_3O_4) nanoparticles were used. The researchers found that at a high Rayleigh number (Ra = 106), the average Nusselt number increased by 75.92%, indicating that the water-Fe_3O_4 nanofluid achieved a higher heat transfer rate, with a maximum increase of 22.65% compared to the base fluid. This research sheds light on the potential of using nanofluids in enhancing heat transfer in various engineering applications. Hirpho et al. [30] simulated the mixed convection of a Casson hybrid nanofluid in a partially heated enclosure using the finite element method and considered the use of an Al_20_3-Cu hybrid nanofluid. The results indicated that the flow function decreased to a certain extent with an increase in the volume percentage of hybrid nanoparticles. The size distribution and design of nanoparticles were found to play a crucial role in heat transfer, which was also observed in a study by Uddin et al. [31]. In their research, they analyzed the convection and flow of a water-copper oxide nanofluid in a symmetrical isosceles triangular cavity with an undulating base wall using a dynamic model.

In recent years, researchers have been focusing on enhancing heat transfer in enclosures by incorporating fins attached to the walls. Zaim et al. [32] conducted a study on the natural convection of a Cu-H_2O Newtonian nanoliquid in a U-shaped enclosure with a single-phase homogeneous nanofluid model under the influence of magneto-hydrodynamic flow (MHD). They observed that the heat transfer rate increased with increasing Rayleigh number and volume fraction and decreased with increasing Hartmann number.

In another study, Rahmati et al. [33] used the Boltzmann lattice method to investigate the natural convection of water-TiO_2 nanofluid in a square cavity with a hot obstacle. They found that increasing the dimensions of the obstacle to 0.5 L resulted in an increase in the average Nusselt number, while increasing it to 0.7 L led to a decrease in the average Nusselt number.

Ma et al. [34, 35] conducted numerical simulations using the Boltzmann lattice method (LBM) to study the natural convection of nanofluids and MHD nanofluids in different geometries. They investigated the natural convection of Al_2O_3-water and TiO_2-water nanofluids in a U-shaped cavity with a heating obstacle and the natural convection of CuO nanofluids in an enclosure with baffles. The study revealed that increasing the Rayleigh number and nanoparticle solid volume fraction (ϕ) increased the average Nusselt number of the obstacle sides, regardless of the aspect ratio. Moreover, increasing the aspect ratio also led to an increase in the average Nusselt number. At low Rayleigh numbers, the effect of nanoparticles on heat transfer enhancement was more pronounced in thin cavities than in large cavities.

Farooq et al. [36] investigated the influence of an external magnetic field on the natural convection hydrothermal characteristics of a non-Newtonian power-law nanofluid in a U-shaped enclosure with baffles. They analyzed the impact of various parameters, such as Rayleigh number (Ra), Hartmann number (Ha), nanoparticle volume fraction (ϕ), cold baffle aspect ratio (AR), inclination angle, and power index (n) on flow and heat transfer. On the other hand, Al-Sayagh [37] conducted a free convection study in a 3D enclosure filled with Al_2O_3 nanofluid and featuring a perfectly conducting U-shaped obstacle. Their results showed that the obstacle's size and orientation could manipulate the flow and optimize the heat transfer, and the addition of nanoparticles notably increased the Nusselt number.

In their numerical investigation, Ali et al. [38] studied a mixed convective flow in a horizontal channel with baffles located alternately on two walls and an external magnetic field. The study revealed that the orientation and height of the baffles significantly influenced the fluid flow and heat transfer. They also found that the heat transfer enhancement decreased by 22.14% at Ha = 50 compared to Ha = 0, and the heat transfer rate was 33.86% higher in a nanofluid containing 5% nanoparticles than in water.

Al-Tahaineh et al. [39] examined a thermoelectric generator (TEG) performance supplemented by an evacuated-tube hydronic solar collector heat exchanger used to heat a cold zone. They found that in addition to the emphasis on improving TEG efficiency, the electricity quantity produced can be significant when large-area heat exchangers are employed in big systems.

Experimental and theoretical investigation of the heat transfer characteristics of a cylindrical heat pipe using Al_2O_3-SiO_2/W-EG hybrid nanofluids by response surface methodology (RSM) was carried out by Vidhya et al. [40]. They concluded that the higher enhancement of the heat pipe's heat transfer characteristics suggested that this new Al_2O_3-SiO_2 hybrid nanofluid could be a surrogate for heat transfer applications in different strategies. Rao et al. [41] showed in their study that the addition of nanoparticles to biodiesel has affirmative impacts in decreasing dangerous emissions such as carbon black, smoke opacity, and NOX, with enhanced thermal efficiency and fuel consumption.

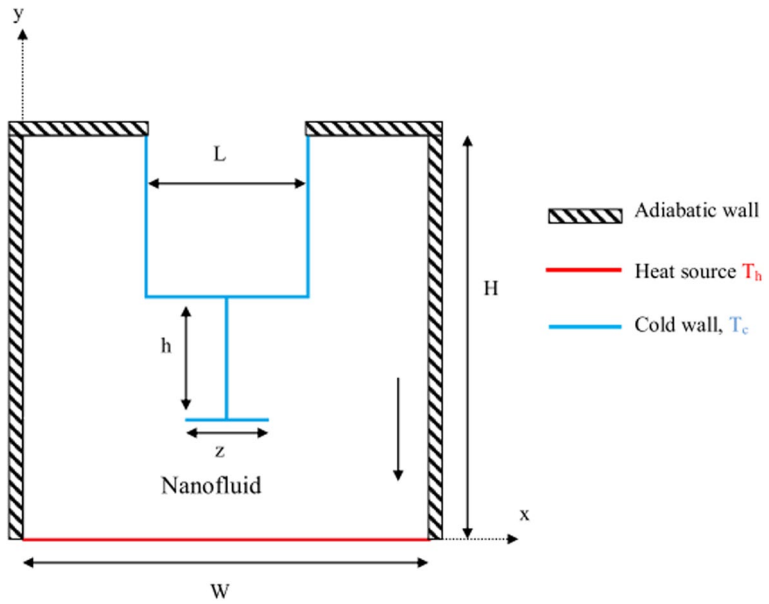

Fig. 1 Schematics and boundary conditions of the case study

The improvement in thermal performance of a twin-tube counter flow heat exchanger with variation in bumper position was investigated experimentally and numerically by Abdul Hussein et al. [42]. Nusselt number and friction factor values were found to be best with the semi-circular bumpers presence compared with the smooth tube. Zhang et al. [43] performed a multi-objective optimization to obtain the optimal cross-finned heat sink design. They revealed that the methodology can ably reduce the computational or experimental costs for the cross-finned heat sink design with increased heat transfer performance and reduced weight.

Based on the related research, it can be concluded that the use of nanofluid-filled enclosures with baffles and obstacles is an attractive option for the efficient cooling of electronic equipment and has been a popular research topic. The current work is an extension of previous research [35], focusing on the effect of a T-shaped baffle placed in the cold rib of a cavity with thermally insulated walls. The active part of the bottom wall is heated to a higher temperature than the top wall. The goal of this analysis is to assess the heat transfer characteristics of this new baffle shape at different Ra numbers, aspect ratios, and nanoparticle concentrations. The simulations are conducted for aspect ratios of 0.4 and 0.6, Ra numbers ranging from 10^4 to 10^6, and nanoparticle concentrations varying from 0 to 0.05, in order to comprehensively explore the impact of these parameters.

Analysis and modeling

Figure 1 displays a U-shaped enclosure with a height (H) and width (W) of 1. The aspect ratios (AR) of its length (L) to height (H) and width (W) are 0.4 and 0.6, respectively. The enclosure is filled with CuO/water nanofluid, and the upper cold wall has a width of L. A T-shaped baffle, which is h units high and z units long (where $h/L = 0.3$ and $z = L/2$), is placed in the middle of the upper cold wall. The upper cold wall and the bottom wall are kept at constant temperatures T_c and T_h, respectively,

while the other walls are adiabatic. The Boussinesq approximation is applied for the nanofluid density variation and other thermo-physical properties. Viscous dissipation effects and velocity differences between the layers are not taken into consideration and the exchange of thermal energy between the nanoparticles and the base fluid is assumed to be negligible.

The continuity, momentum, and energy equations are as given:

$$\frac{\partial U}{\partial X}+\frac{\partial V}{\partial Y}=0 \tag{1}$$

$$U\frac{\partial U}{\partial X}+V\frac{\partial U}{\partial Y}=-\frac{\partial P}{\partial X}+\frac{\mu_{nf}}{\rho_{nf}\alpha_f}\left[\frac{\partial^2 U}{\partial X^2}+\frac{\partial^2 U}{\partial Y^2}\right] \tag{2}$$

$$U\frac{\partial V}{\partial X}+V\frac{\partial V}{\partial Y}=-\frac{\partial P}{\partial y}+\frac{\mu_{nf}}{\rho_{nf}\alpha_f}\left[\frac{\partial^2 U}{\partial X^2}+\frac{\partial^2 U}{\partial Y^2}\right]+\frac{(\rho\beta)_{nf}}{\rho_{nf}\beta_f}Ra.\Pr.\theta \tag{3}$$

$$U\frac{\partial \theta}{\partial X}+V\frac{\partial \theta}{\partial Y}=\frac{\alpha_{nf}}{\alpha_f}\left(\frac{\partial^2 \theta}{\partial X^2}+\frac{\partial^2 \theta}{\partial Y^2}\right) \tag{4}$$

$$Ra\frac{g\beta_f L^3\triangle L}{V_f\alpha_f}\text{ and }\Pr=\frac{V_f}{\alpha_{\mathrm{f}}}\quad X=\tfrac{x}{L}\,,\ Y=\tfrac{y}{L}\,,\ U=\tfrac{uL}{\alpha_f}\,,\ V=\tfrac{vL}{\alpha_f}\quad P=\tfrac{pL}{\rho_f{\alpha_f}^2}\,,\ \theta=\tfrac{T-T_c}{\triangle T}\,,\ \triangle T=T_h-T_c$$

$$Nu_{local}=\frac{hL}{k_f} \tag{5}$$

$$h=\frac{q}{T_h-T_c} \tag{6}$$

Where q is the heat flux on the hot wall.

The average Nusselt number [35].

$$Nu_{ave}=\int\limits_{Bottomwall} Nu_{local}\,dX|_{Y=0}=\int\limits_{Bottomwall}\frac{k_{nf}}{k_f}\frac{\partial T}{\partial n}dX|_{Y=0} \tag{7}$$

Table 1 displays the thermophysical properties of the nanofluid, including density, specific heat, thermal expansion coefficient [44], dynamic viscosity, and thermal

Table 1 Characterization of the thermophysical properties of investigated materials [12]

	ρ (kg/m^3)	C_p ($J/kg.k$)	k ($W/m.k$)	β ($1/k$)
Pure water	997.1	4179	0.613	21×10^{-5}
CuO	6500	540	18	1.67×10^{-5}

conductivity. The Table 2 shows the applied formulation for the nanofluid properties, the thermal conductivity was determined using both the Maxwell method [45] and Brinkman [46] technique.

Methods

The pressure-based solver and finite-volume method (FVM) based code was used to solve the Navier–Stokes equations in this study. The SIMPLE algorithm was employed to relate the velocity and pressure-based, and the second-order upwind method was adopted to discretize the governing equations. To ensure a converged solution, the convergence criterion for continuity, momentum, and energy residuals were reduced. No-slip boundary conditions were applied throughout the simulation. Several grids were created to examine the size effect, and the average Nusselt number variation on the hot wall was observed for the case of Ar = 0.4, ϕ = 0.05 (Table 3). The entire calculations were carried out using a 300×300 mesh to ensure a mesh-independent solution. The

Table 2 Applied formulation for the nanofluid properties

Nanofluid properties	Applied model
Density	$\rho_{nf} = (1-\phi)\rho_f + \phi\rho_p$
Specific heat	$(\rho C_p)_{nf} = (1-\phi)(\rho C_p)_f + \phi(\rho C_p)_p$
Thermal diffusivity	$\alpha_{nf} = k_{nf}/(\rho C_p)_{nf}$
Thermal expansion coefficient	$(\rho\beta)_{nf} = (1-\phi)\rho_f + \phi\rho_p$
Dynamic viscosity	$\mu_{nf} = \frac{\mu_f}{(1-\phi)^{2.5}}$
Thermal conductivity	$k_{nf} = k_f\left[\frac{(k_p+2k_f)-2\phi(k_f-k_p)}{(k_p+2k_f)+\phi(k_f-k_p)}\right]$

Table 3 Influence of grid resolution on average Nusselt number for Ar = 0.4, φ = 0.05

Ra	Number of nodes	Average Nusselt number	Percentage of error $\left\lvert\frac{Nu_{new}-Nu_{previous}}{Nu_{new}}\right\rvert \times 100$
10^4	100×100	2.3479	-
	200×200	2.33776	0.04363
	300×300	2.3240	**0.059208**
	400×400	2.2958	0.012283
10^5	100×100	7.96360	-
	200×200	7.56556	0.12557
	300×300	7.7013	**0.01762**
	400×400	7.9542	0.03179
10^6	100×100	15.9035	-
	200×200	15.0586	0.056107
	300×300	14.8579	**0.013507**
	400×400	15.9324	0.067497

precision of the numerical results obtained in this study was confirmed by comparing the simulation with the numerical results obtained in previous research [35], which used CuO water nanofluid and the same cavity. Table 4 shows that the consistency between the results obtained in this study and the literature is quite good.

Results and discussion

In order to investigate the flow characteristics of the nanofluid, several parameters were varied, including nanoparticle volume fractions ranging from 0 to 0.05, Rayleigh numbers of 10^4, 10^5, and 10^6, and two different aspect ratios of 0.4 and 0.6. The T-shaped baffle positioned at the center of the cold slot on the bottom wall is considered.

Figures 2, 3, 4, and 5 illustrate the impact of the Rayleigh number on both isotherms and streamlines. As seen in Figs. 2 and 4, when the Rayleigh number is higher than 10^4, the isotherm lines are located closer to the cold groove. However, for Rayleigh numbers 10^5 and 10^6, the isotherms undergo significant variations, with those close to the hot wall bending and those close to the cold groove following the T-shaped baffle's geometric pattern and adopting the shape of the groove. This behavior can be attributed to the increase in the buoyant force associated with Rayleigh's growth. As

Table 4 Comparison of the average Nusselt number for Ra = 105 and φ = 0.05 in the current study and [35]

Aspect ratio	Nu (present study)	Nu (Ma et al. [35])	Percentage of error $\left\lvert \frac{Nu_{present} - Nu_{litterature}}{Nu_{present}} \right\rvert \times 100$
Ar = 0.4	9.0328	9.1847	**0.01681**
Ar = 0.6	9.3816	9.5108	**0.01377**

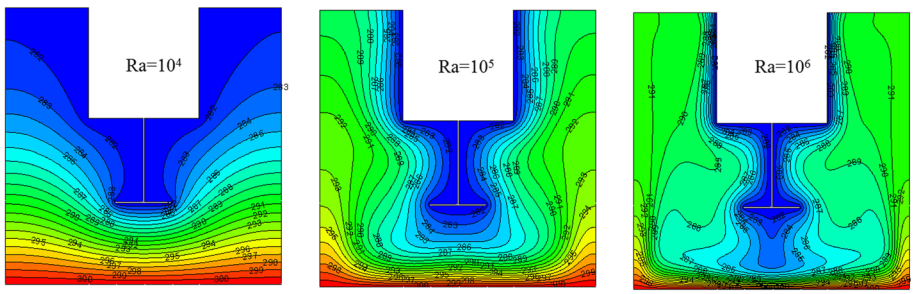

Fig. 2 Isotherms at different Ra for Ar = 0.4 φ = 0.05

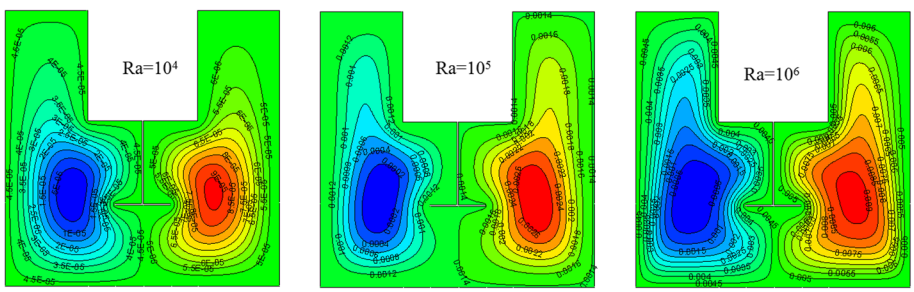

Fig. 3 Streamlines at different Ra for Ar = 0.4 φ = 0.05

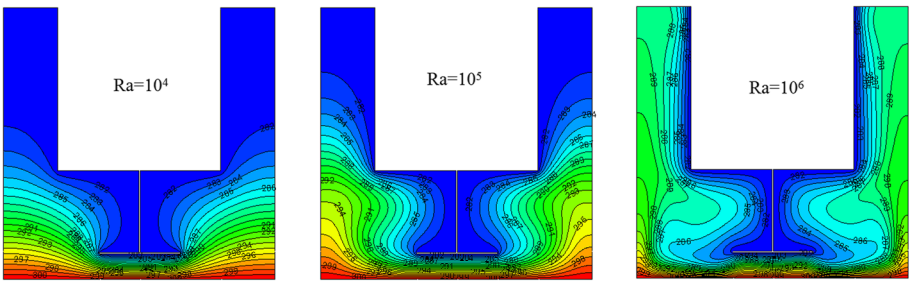

Fig. 4 Isotherms at different Ra for Ar = 0.6 φ = 0.05

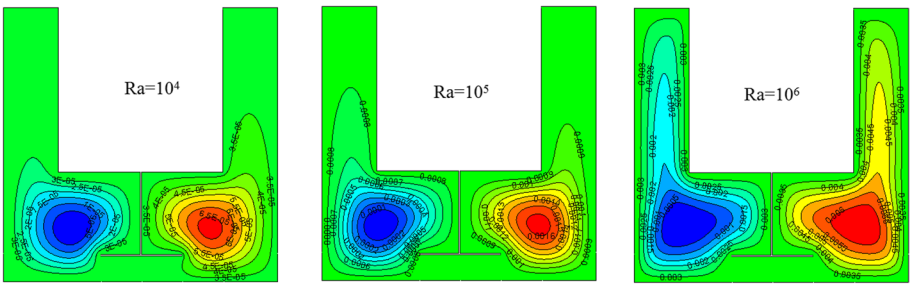

Fig. 5 Streamlines at different Ra for Ar = 0.6 φ = 0.05

the Rayleigh number increases, the buoyant force becomes stronger, which causes the fluid to circulate more vigorously. Consequently, this improves heat transfer as the fluid carries heat more efficiently from the hot surface to the cold surface. Overall, these findings suggest that the Rayleigh number plays a crucial role in determining the heat transfer characteristics of the nanofluid and that the T-shaped baffle has a significant impact on the flow patterns and heat transfer in the system.

The results revealed that two distinct thermal panaches occur above the right and left sides of the hot wall. The resulting thermal plumes then enter the cold groove, which reduces the boundary layer thickness above the cold walls. At lower Rayleigh numbers, such as $Ra = 10^4$, the conductive heat transfer mechanism is more pronounced. However, at higher Rayleigh numbers ($Ra = 10^5$–10^6), the convective heat transfer mechanism becomes more significant and takes over from conduction. This shift can be attributed to the enhancement of buoyancy forces on the fluid particles as the Rayleigh number increases. The buoyancy forces promote the movement of the fluid particles, which in turn reduces the thermal boundary layer thickness and enhances convective heat transfer. As a result, heat transfer improves as Ra increases. Overall, these findings highlight the interplay between conductive and convective heat transfer mechanisms and the critical role played by buoyancy forces in determining the heat transfer characteristics of the nanofluid.

In Figs. 3, 4, and 5, two clockwise and counterclockwise vortices are visible on the right and left sides of the enclosure. These vortices are caused by the presence of the baffle. Specifically, the fluid adjacent to the bottom wall is hot, and the temperature difference generates a buoyancy force that causes the fluid in the cavity to rise. However, the baffle disrupts this movement, resulting in the formation of two recirculation areas.

Overall, the baffle plays a crucial role in determining the flow patterns in the system. It restricts the fluid's movement, which creates vortices and recirculation areas. These features have a significant impact on the heat transfer characteristics of the nanofluid and highlight the importance of considering the effects of baffle presence when designing and analyzing heat transfer systems.

Increasing the Rayleigh number (Ra) leads to an increase in buoyancy forces, which draws the streamlines toward the walls due to the higher fluid velocity near the walls. In addition, the two peaks become larger and stronger with a Rayleigh number of 10^6. The effects of aspect ratio (AR) and nanoparticles volume fraction (ϕ) on isotherms and streamlines at $Ra = 10^5$ are shown in Figs. 6 and 7, respectively. Figure 6 shows that increasing the aspect ratio leads to a decrease in fluid temperature in both sections due to the restriction of fluid motion. This results in more compact isotherms near the bottom wall, reducing the thickness of the thermal boundary layer. Thus, increasing the aspect ratio enhances the temperature gradient near the hot wall. The isotherms near the cold wall still have the form of the cold wall and T-shaped baffle at $AR = 0.4$, while at $AR = 0.6$, the isotherms continue with the baffle shape for any ϕ due to the strengthening of the spacing effect on flux limitation and heat transfer at a large aspect ratio. The addition of nanoparticles has a negligible impact on temperature distribution except for around the hot wall, where the temperature rises. Increasing the nanoparticles volume fraction leads to a growth in the thickness of the thermal boundary layer above the hot wall. Overall, these findings highlight the complex interplay between various parameters in determining the heat transfer characteristics of the nanofluid system and emphasize the need for a comprehensive understanding of the underlying physics for optimal system design and performance.

Based on the information provided in Fig. 7, it can be observed that for an aspect ratio of 0.4 and any nanoparticle volume fraction, two vortices are formed in the clockwise

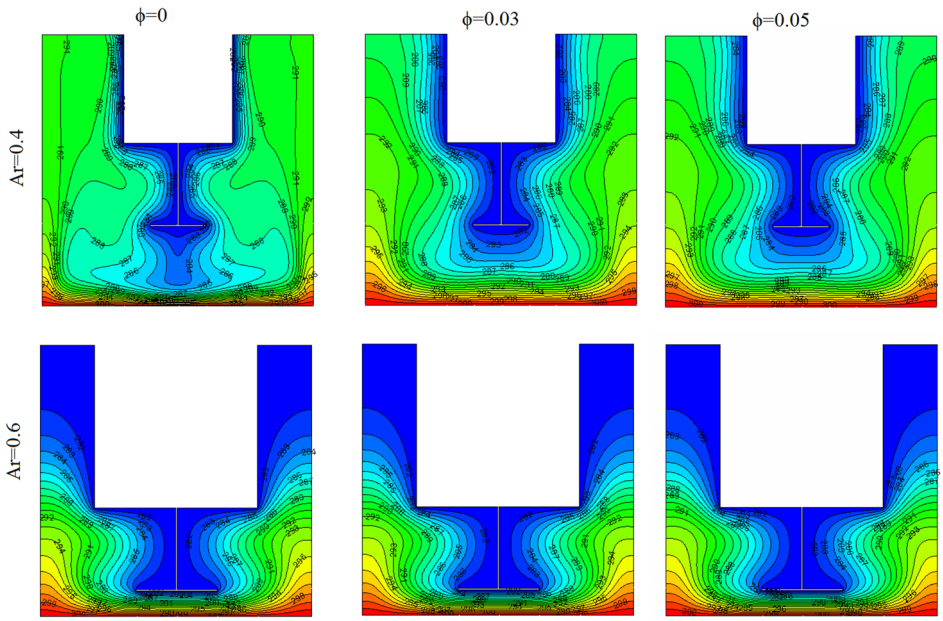

Fig. 6 Isotherms at different φ and Ar for $Ra = 10.^5$

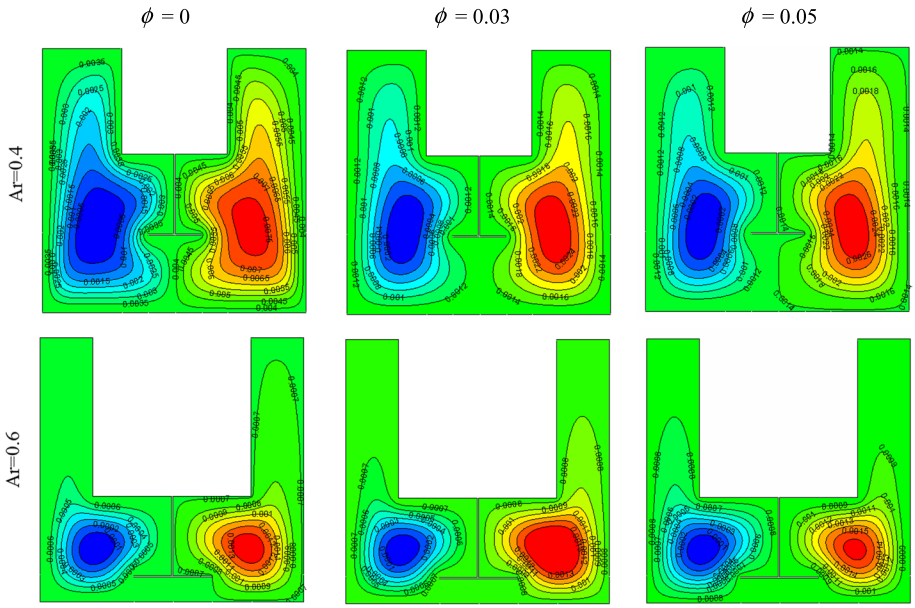

Fig. 7 Streamlines at different φ and Ar for Ra = 10^5

and anticlockwise directions due to buoyancy forces. Natural convection is the dominant mode of heat transfer, and the eddy rings formed have a circular shape. On the other hand, for an aspect ratio of 0.6, the eddy rings become elliptical in shape. However, the addition of nanoparticles to the fluid does not significantly affect the streamlined pattern, even when the nanoparticle volume fraction is increased from 0 to 0.03.

In Fig. 8, the distribution of local Nusselt numbers along the hot wall is presented for various Rayleigh numbers and aspect ratios at a fixed nanoparticle volume fraction of 0.05. It is observed that an increase in the Rayleigh number leads to an increase in the value of the local Nusselt number, and the contour of the local Nusselt number changes significantly as the aspect ratio is increased. The local Nusselt number profile on the hot wall is symmetric with respect to the middle horizontal line, has an arc shape, and the peak value of the local Nusselt number is located at the position of the baffle. Furthermore, as the aspect ratio is increased, the local Nusselt number profile rises and the curvature profile also increases. Notably, when the aspect ratio is increased from 0.4 to 0.6, the contour of the local Nusselt number profile is significantly altered.

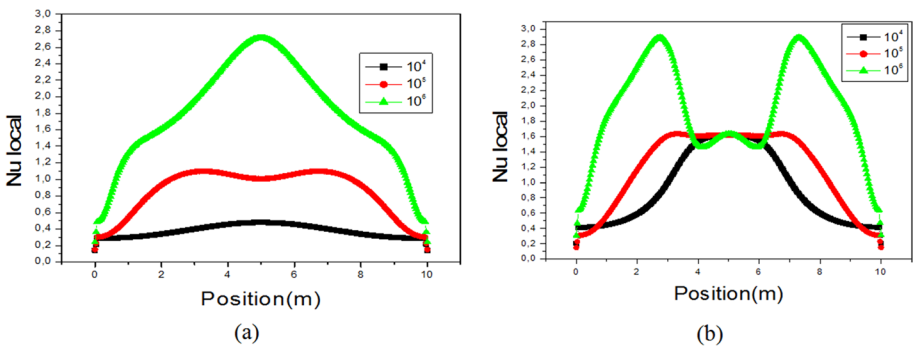

Fig. 8 Local Nusselt number for φ = 0.05 and different Ra. **a** Ar = 0.4, **b** Ar = 0.6

To summarize, Figs. 9, 10, and 11 show the effects of Rayleigh number and nanoparticle volume fraction on the mean Nusselt number for both aspect ratios. It is observed that the mean Nusselt number is higher at AR = 0.6 than at AR = 0.4. The variation trends of the mean Nusselt number as a factor of nanoparticle volume fraction and Rayleigh number are similar for both aspect ratios, and increasing the Rayleigh number leads to a significant increase in the Nusselt number due to the dominance of the convection mechanism over the conduction mechanism at higher Rayleigh numbers. On the other hand, the nanoparticle volume fraction does not significantly affect the Nusselt number.

Table 5 shows the comparison of average Nusselt number values for the U-shaped cavity without a baffle, with a straight baffle, and with a T-shaped baffle at different Rayleigh numbers. It can be observed that the T-shaped baffle significantly enhances the heat transfer rate compared to the other two cases. For instance, at $Ra = 10^6$, the average Nusselt number for the T-shaped baffle case is 20.59% higher than that for the cavity without baffle, at $Ra = 10^4$, the average Nusselt number for the T-shaped baffle case is 61.58% higher than that for the straight baffle case, and at $Ra = 10^5$, it is 78.21% higher than that for the cavity without baffle. This indicates that the T-shaped baffle is effective in improving the convective heat transfer in the U-shaped cavity. Furthermore, Fig. 12 shows the average Nusselt number variation in the U-shaped cavity with a T-shaped baffle at different Rayleigh numbers. It can be observed that the temperature difference between the hot and cold walls increases with increasing Rayleigh number, indicating the enhancement of the convective heat transfer mechanism. The T-shaped baffle can also be seen to create strong vortices and recirculation zones, which promote the heat transfer rate.

Conclusions

A study was conducted to investigate the natural convection of a CuO-water nanofluid in a U-shaped enclosure with a T-shaped baffle through numerical simulation. Various parameters were considered, including the cavity aspect ratios of 0.4 and 0.6, Ra

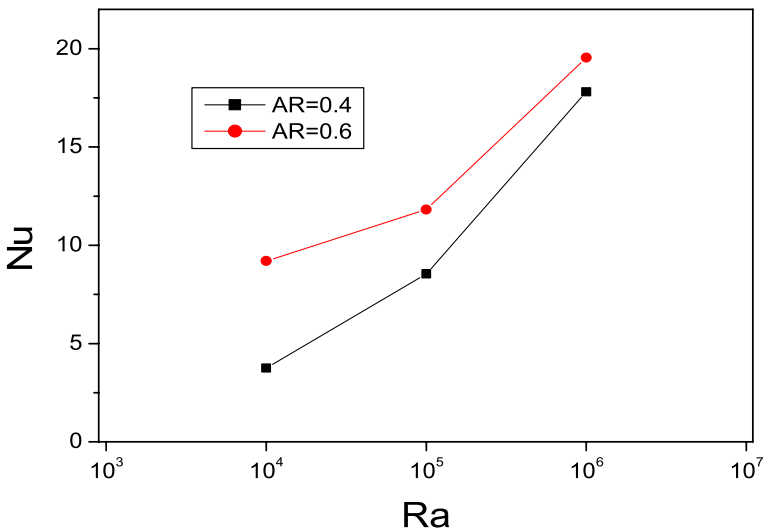

Fig. 9 Nusselt number variation versus Ra for different Ar at $\varphi = 0.05$

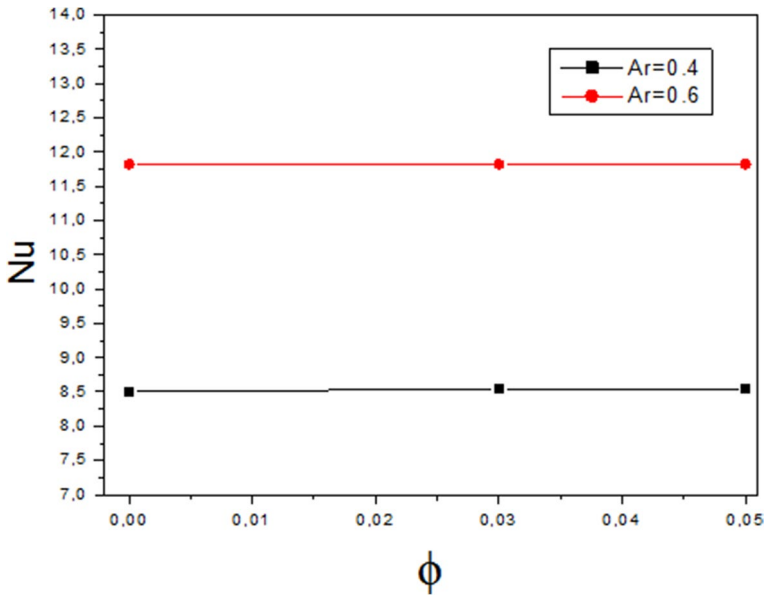

Fig. 10 Average Nusselt number versus φ for different Ar at Ra = 10^5

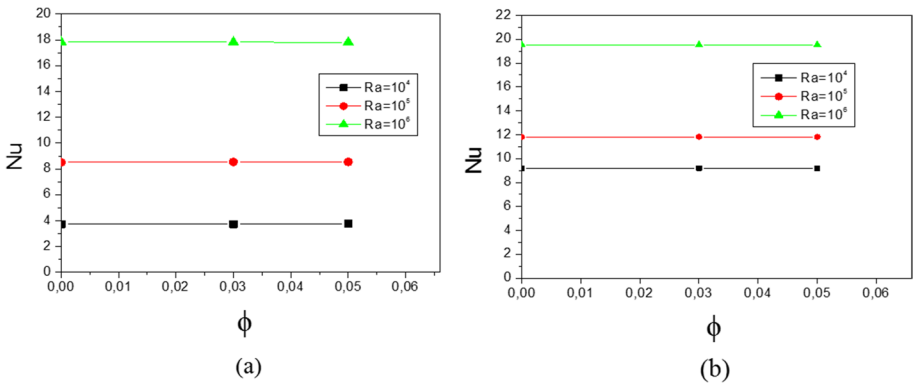

Fig. 11 Average Nusselt number versus φ for different Ra. **a** Ar = 0.4, **b** Ar = 0.6

Table 5 Average Nusselt number variation at different Ra for Ar = 0.6 and φ = 0.05

Ra	Nu_m (without baffle)	Nu_m (straight baffle)	Nu_m (T-shaped baffle)
10^4	3.6863	5.6951	9.2026
10^5	6.6313	8.9328	11.8182
10^6	16.6029	18.5878	19.5398

numbers ranging from 10^4 to 10^6, and nanoparticle volumetric concentrations of 0 to 0.05. The results indicate the following:

- Increasing Ra leads to an enhancement of the heat transfer ratio and a reduction in the thickness of the thermal boundary layer due to increased buoyancy forces. Moreover, high Rayleigh numbers (Ra $\geq 10^4$) significantly increase the heat transfer ratio.

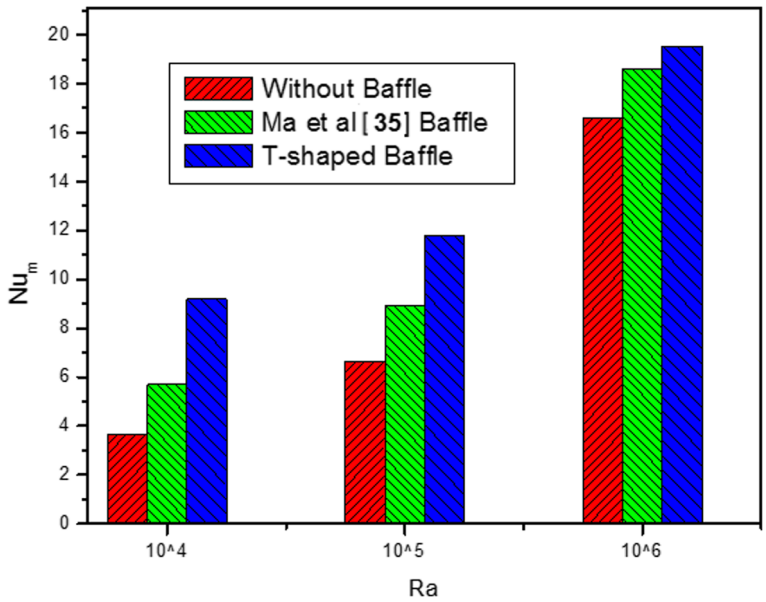

Fig. 12 Average Nusselt number variation versus Rayleigh number with different baffle shapes for Ar = 0.6 and $\varphi = 0.05$

- The inclusion of nanoparticles also enhances the heat transfer ratio, and an increase in nanoparticle volumetric concentration (ϕ) leads to an increase in the Nusselt number.
- The aspect ratio shift may not alter the flow pattern; an increase in aspect ratio (Ar) improves the heat transfer rate.
- The T-shaped baffle improves the heating performance at AR = 0.6 and $\phi = 0.05$, and the heat transfer enhancement is largely influenced by the Rayleigh number at a high aspect ratio.
- The heat transfer is significantly better for the T-shaped baffle compared to other baffles, with an improvement of 61.58% compared to the straight baffle at $Ra = 10^4$ and 78.21% compared to the cavity without baffle at $Ra = 10^6$.
- This study offers valuable recommendations for the development of non-square geometries and high thermal-performance media storage. The findings can be applied to various industries such as car radiators, U-tube heat exchangers, tank-to-tank connectors, cooling in double baffle space, and nuclear reactors.

Abbreviations

AR	Aspect ratio
g	Gravitational acceleration (m/s^2)
H	Height of enclosure (m)
w	Height of baffle (m)
L	Width of the enclosure (m)
Nu	Nusselt number
P	Pressure (N/m^2)
Pr	Prandtl number
Ra	Rayleigh number
T	Temperature (K)
ΔT	Temperature variation, T_h–T_c (k)
U	Velocity component in x-direction (m/s)
V	Velocity component in y-direction (m/s)
X,Y	Dimensionless coordinates

z Baffle length (m)

Greek symbols

k Thermal conductivity of fluid (W/m k)
α Thermal diffusivity (m^2/s)
β Coefficient of volumetric expansion (1/K)
θ Dimensionless temperature, (T–To)
μ Dynamic viscosity (N s/m^2)
ρ Fluid density (kg/m^3)
φ Volume fraction

Subscripts

c Cold
h Hot
nf Nanofluid
f Fluid
p Solid particles
0 Initial
m Mean

Acknowledgements
The authors thank the reviewers for their valuable suggestions in improving the manuscript.

Authors' contributions
F. Zemani conceived of the presented idea, developed the theory, performed the computations, and contributed to the final version of the manuscript. O. Ladjedel performed the analytic calculations and the numerical simulations. A. Sabeur developed the theoretical formalism, discussed the results, and contributed to the final manuscript. The authors have read and approved the final manuscript.

Funding
This research acquired no explicit funding from any government, commercial, or not-for-profit organization.

Availability of data and materials
The data acquired and/or evaluated during the present research are accessible upon valid request from the corresponding author.

Declarations

Competing interests
The authors declare that they have no competing interests.

Received: 5 April 2023 Accepted: 14 July 2023
Published online: 22 August 2023

References

1. Choi SUS (1995) Enhancing thermal conductivity of fluids with nanoparticles. in: D.A. Siginer, H.P. Wang (Eds.), Developments and Applications of Non-Newtonian Flows, FED-Vol. 231 , pp. 99–105 66
2. Trisaksri V, Wongwises S (2007) Critical review of heat transfer characteristics of nanofluids. Ren Sust En Rev 11:512–523
3. Khanafer K, Vafai K, Lightstone M (2003) Buoyancy-driven heat transfer enhancement in a two-dimensional enclosure utilizing nanofluids. Int J Heat Mass Transfer 46:3639–3653. https://doi.org/10.1016/S0017-9310(03)00156-X
4. Putra N, Roetzel W, Das SK (2003) Natural convection of nanofluids. Heat Mass Transfer 39:775–784
5. Chon CH, Kihm KD, Lee SP, Choi SUS (2005) Empirical correlation finding the role of temperature and particle size for nanofluid (Al_2O_3) thermal conductivity enhancement. Appl Phys Lett 87:153107
6. Daungthongsuk W, Wongwises S (2007) A critical review of convective heat transfer nanofluids. Ren Sust En Rev 11:797–817
7. Abu-Nada E, Masoud Z, Oztop HF, Campo A (2010) Effect of nanofluid variable properties on natural convection in enclosures. Int J Therm Sci 49:479–491. https://doi.org/10.1016/j.ijthermalsci.2009.09.002
8. Aminossadati SM, Ghasemi B (2009) Natural convection cooling of a localized heat source at the bottom of a nanofluid filled enclosure. Eur J Mechanics B/Fluids 28:630–640. https://doi.org/10.1016/j.euromechflu.2009.05.006
9. Cho CC, Yau HT, Chen CK (2012) Enhancement of natural convection heat transfer in a U-shaped cavity filled with Al_2O_3-water nanofluid. Therm Sci 16(5):1317–1323. https://doi.org/10.2298/TSCI1205317C
10. Abu-Nada E, Chamkha AJ, (2010) Effect of nanofluid variable properties on natural convection in enclosures filled with a CuO-EG-Water nanofluid. Int J Thermal Sci 49: 2339e2352. https://doi.org/10.1016/j.ijthermalsci.2010.07.006
11. Ghasemi B, Aminossadati SM (2009) Natural convection heat transfer in an inclined enclosure filled with a water-Cuo nanofluid, numerical heat transfer. Part A: Applications Int J Computation Methodol 55(8):807–823. https://doi.org/10.1080/10407780902864623

12. Ghasemi B, Aminossadati SM, Raisi A (2011) Magnetic field effect on natural convection in a nanofluid-filled square enclosure. Int J Thermal Sci 50:1748 e 1756. https://doi.org/10.1016/j.ijthermalsci.2011.04.010
13. Oztop HF, Abu-Nada E (2008) Numerical study of natural convection in partially heated rectangular enclosures filled with nanofluids. Int J Heat Fluid Flow 29:1326–1336. https://doi.org/10.1016/j.ijheatfluidflow.2008.04.009
14. Srinivas Rao S, Srivastava A (2016) Interferometric study of natural convection in a differentially-heated cavity with Al_2O_3 –water based dilute nanofluids. Int J Heat Mass Transf 92:1128–1142. https://doi.org/10.1016/j.ijheatmasstransfer.2015.09.074
15. Yıldız Ç, Arıcı M, Karabay H (2019) Effect of inclination angle on natural convection of nanofluids in a U-shaped cavity. Int J Environ Sci Technol 16:5289–5294. https://doi.org/10.1007/s13762-019-02407-2
16. Yıldız Ç, Arıcı M, Karabay H, andBennacer R, (2020) Natural convection of nanofluid in a U-shaped enclosure emphasizing on the effect of cold rib dimensions. J Therm Anal Calorim. https://doi.org/10.1007/s10973-020-10023-3
17. Mohebbi R, Izadi M, Sajjadi H, Delouei AA, Sheremet MA (2019) Examining of nanofluid natural convection heat transfer in a Γ-shaped enclosure including a rectangular hot obstacle using the lattice Boltzmann method. Physica A 526:120831. https://doi.org/10.1016/j.physa.2019.04.067
18. Chamkha A, Ismael M, Kasaeipoor, Armaghani T (2016) Entropy generation and natural convection of CuO-water nanofluid in C-shaped cavity under magnetic field. Entropy 18: 50. https://doi.org/10.3390/e18020050
19. Mahalakshmi T, Nithyadevi N, Oztop HF, Abu-Hamdeh N (2018) Natural convective heat transfer of Ag-water nanofluid flow inside enclosure with center heater and bottom heat source. Chin J Phys. https://doi.org/10.1016/j.cjph.2018.06.006
20. Triveni MK, Sen D, Panua R (2016) Numerical study of laminar natural convection in an arch enclosure filled with Al_2O_3 -water based nanofluid. J Appl Fluid Mechanics 9(4):1927–1936. https://doi.org/10.18869/acadpub.jafm.68.235.24798
21. Dutta S, Biswas AK (2019) A numerical investigation of natural convection heat transfer of copper-water nanofluids in a rectotrapezoidal enclosure heated uniformly from the bottom wall. Mathematical Model Eng Problems 6(1):105–11. https://doi.org/10.18280/mmep.060114
22. Snoussi L, Ouerfelli N, Chesneau X, Chamkha AJ, Bin Muhammad Belgacem F, Guizani A (2018) Natural convection heat transfer in a nanofluid filled U-shaped enclosures: numerical investigations, heat transfer engineering. 39;(16). https://doi.org/10.1080/01457632.2017.1379343
23. Islam S, Bairagi T, Islam T, Rana BMJ, Reza-E-Rabbi SK, Rahman MM (2022) Heatline visualization in hydromagnetic natural convection flow inside a prismatic heat exchanger using nanofluid. Int J Thermofluids 16:100248
24. Hasan MJ, Azad AK, Islam Z, Hossain R, Rahman MM (2022) Periodic unsteady natural convection on CNT nanopowder liquid in a triangular shaped mechanical chamber. Int J Thermofluids 15:100181
25. Astanina MS, Sheremet MA (2023) Numerical study of natural convection of fluid with temperature-dependent viscosity inside a porous cube under non-uniform heating using local thermal non-equilibrium approach. Int J Thermofluids 17:100266
26. Kadhim HT, Al-Manea A, Al-Shamani AN, Yusaf T (2022) Numerical analysis of hybrid nanofluid natural convection in a wavy walled porous enclosure: local thermal non-equilibrium model. Int J Thermofluids 15:100190
27. Alam MS, Keya SS, Salma U, Hossain SC, Billah MM (2022) Convective heat transfer enhancement in a quarter-circular enclosure utilizing nanofluids under the influence of periodic magnetic field. Int J Thermofluids 16:100250
28. Al Hajri AR, Rahman MM, Eltayeb IA (2023) Impacts of Maxwell-Cattaneo effects on the convective heat transfer flow inside a square enclosure filled with a porous medium. Int J Thermofluids 17:100254
29. Hasan MM, Uddin MJ, Nasrin R (2022) Exothermic chemical reaction of magneto-convective nanofluid flow in a square cavity. Int J Thermofluids 16:100236
30. Hirpho M, Ibrahim W (2022) Modeling and simulation of hybrid Casson nanofluid mixed convection in a partly heated trapezoidal enclosure. Int J Thermofluids 15:100166.
31. Uddin MJ, Al-Balushi J, Mahatabuddin S, Rahman MM (2022) Convective heat transport for copper oxide-water nanofluid in an isosceles triangular cavity with a rippled base wall in the presence of magnetic field. Int J Thermofluids 16:100195
32. Zaim A, Aissa A, Mebarek-Oudina F, Mahanthesh B, Lorenzini G, Sahnoun M, El Ganaoui M (2020) Galerkin finite element analysis of magneto-hydrodynamic natural convection of Cu-water nanoliquid in a baffled U-shaped enclosure. Propulsion and Power Research. https://doi.org/10.1016/j.jppr.2020.10.002
33. Rahmati AR, Tahery AA (2017) Numerical study of nanofluid natural convection in a square cavity with a hot obstacle using lattice Boltzmann method. Alexandria Eng J https://doi.org/10.1016/j.aej.2017.03.030
34. Ma Y, Mohebbi R, Rashidi MM, Yang Z, (2018) Simulation of nanofluid natural convection in a U-shaped cavity equipped by a heating obstacle: effect of cavity's aspect ratio. J Taiwan Institute Chem Eng 93. https://doi.org/10.1016/j.jtice.2018.07.026
35. Ma Y, Mohebbi R, Rashidi M.M., Yang Z, Sheremet MA (2019) Numerical study of MHD nanofluid natural convection in a baffled U-shaped enclosure. Int J Heat Mass Transfer 130:123–134. https://doi.org/10.1016/j.ijheatmasstransfer.2018.10.072
36. Ali FH, Hamzah HK, Egab K, Arıcı M, Shahsavar A (2020) Non-Newtonian nanofluid natural convection in a U-shaped cavity under magnetic field. Int J Mechanical Sci 186:105887. https://doi.org/10.1016/j.ijmecsci.2020.105887
37. Al-Sayagh R (2021) Control of the free convective heat transfer using a U-shaped obstacle in an Al2O3-water nanofluid filled cubic cavity. Int J Adv Appl Sci 8(7):23–30, https://doi.org/10.21833/ijaas.2021.07.004
38. Ali MM, Akhter R, Miah MM (2021) Hydromagnetic mixed convective flow in a horizontal channel equipped with Cu-water nanofluid and alternated baffles. International Journal of Thermofluids 12:100118
39. Al-Tahaineh H, AlEssa AHM (2022) A hybrid TEG/evacuated tube solar collectors for electric power generation and space heating. J Eng Appl Sci 69:10. https://doi.org/10.1186/s44147-021-00065-1
40. Vidhya R, Balakrishnan T, Kumar BS (2021) Experimental and theoretical investigation of heat transfer characteristics of cylindrical heat pipe using Al_2O_3–SiO_2/W-EG hybrid nanofluids by RSM modeling approach. J Eng Appl Sci 68:32. https://doi.org/10.1186/s44147-021-00034-8

41. Rao MS, Rao CS, Kumari AS (2022) Synthesis, stability, and emission analysis of magnetite nanoparticle-based biofuels. J Eng Appl Sci 69:79. https://doi.org/10.1186/s44147-022-00127-y
42. Abdul Hussein SA, Shbailat SJ (2023) Impact of bumpers position variation on heat exchanger performance: an experimental and predictive analysis using an artificial neural network. J Eng Appl Sci 70:6. https://doi.org/10.1186/s44147-023-00176-x
43. Zhang C, Chen L, Tong Z (2022) Multi-objective optimization of heat sink with multi-cross-ribbed-fins for a motor controller. J Eng Appl Sci 69:34. https://doi.org/10.1186/s44147-022-00085-5
44. Mahmoodi M (2011) Numerical simulation of free convection of a nanofluid in L-shaped cavities. Int J Therm Sci https://doi.org/10.1016/j.ijthermalsci.2011.04.009
45. Maxwell JC (1904) A treatise on electricity and magnetism, 2nd edn. Oxford University Press, Cambridge, pp 435–441
46. Brinkman HC (1952) The viscosity of concentrated suspensions and solutions. J Chem Phys 20:571–581